

Supporting Information

Toward Real-time Monitoring Lithium Metal Growth and Early Dendrite Formation Surveillance for Safe Lithium Metal Batteries

Houchao Zhan,^{a, b} Peichao Zou,^{*a, c} Wentao Yao,^a Long Qian,^{a, b} Kangwei Liu,^{a, b}
Shengyu Hu,^a Haojie Zhu,^a Yanbing He,^a Feiyu Kang,^{a, b} Cheng Yang^{*a}

^a Division of Energy and Environment, Tsinghua Shenzhen International Graduate School, 518055, China.

^b School of Materials Science and Engineering, Tsinghua University, Beijing, 100084, China.

^c Department of Physics and Astronomy, University of California, Irvine, 92697, United States.

*Corresponding authors: yang.cheng@sz.tsinghua.edu.cn, zoupc2019@163.com

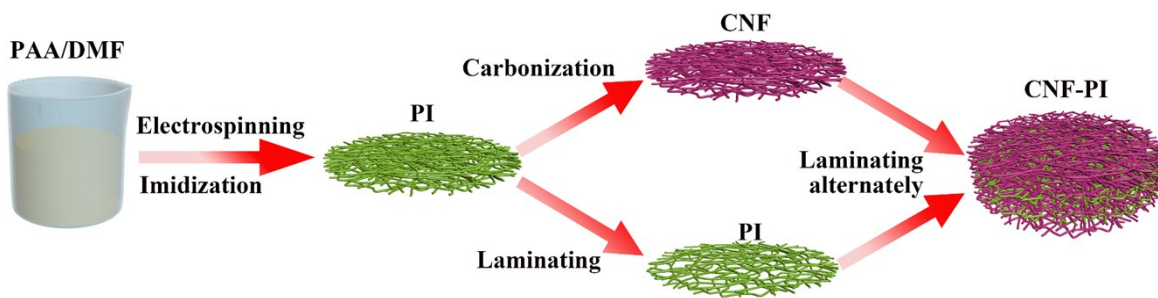


Fig. S1. Schematic diagram of the fabrication process of the CNF-PI host.

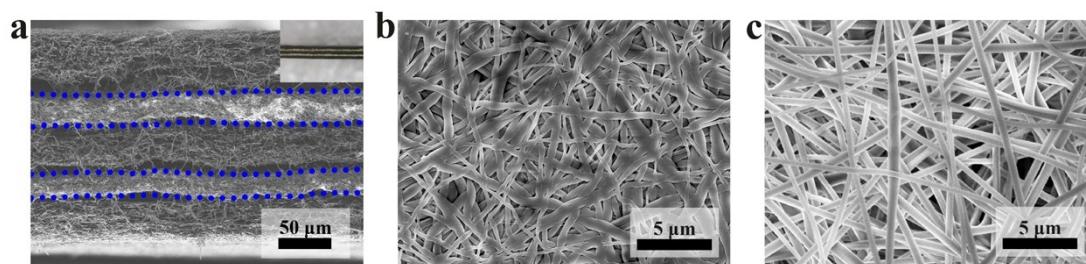


Fig. S2. SEM images of (a) Cross-sectional SEM image of CNF-PI 3D host, (b) PI films after laminating and (c) CNF scaffold. Inset panel in (a) is digital photograph of CNF-PI.

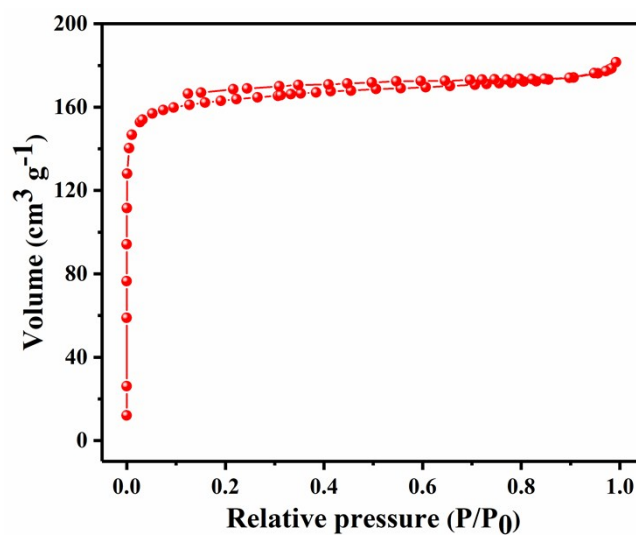


Fig. S3. Nitrogen adsorption-desorption isotherm of CNF.

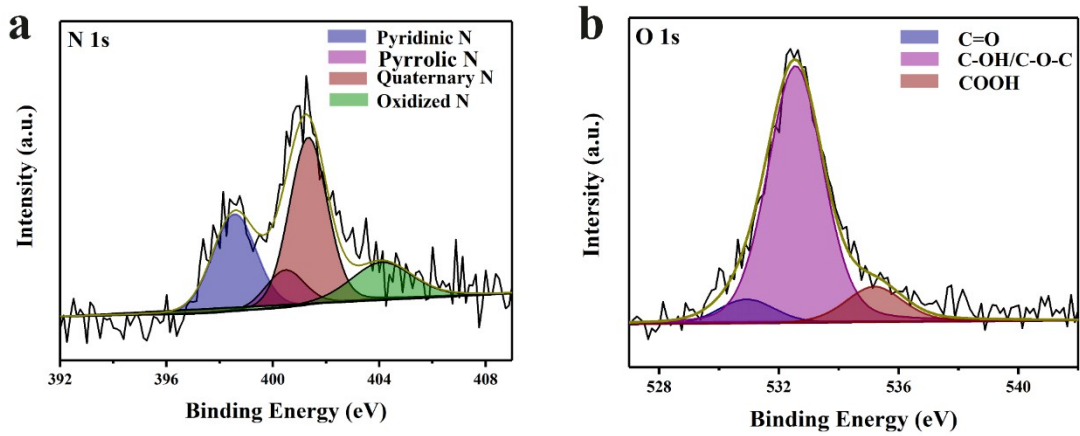


Fig. S4. (a) N 1s and (b) O 1s high-resolution XPS spectra for CNF.

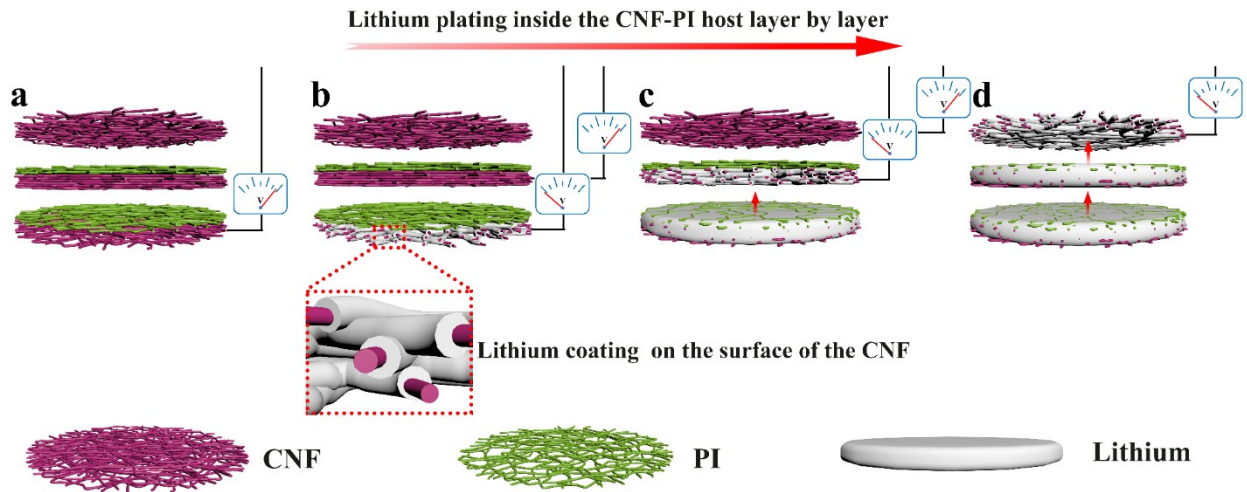


Fig. S5. Schematic illustration of the lithium plating process inside the CNF-PI host. Lithium metal grow in a stepwise “bottom-up” manner due to the block of the electronic transport path.

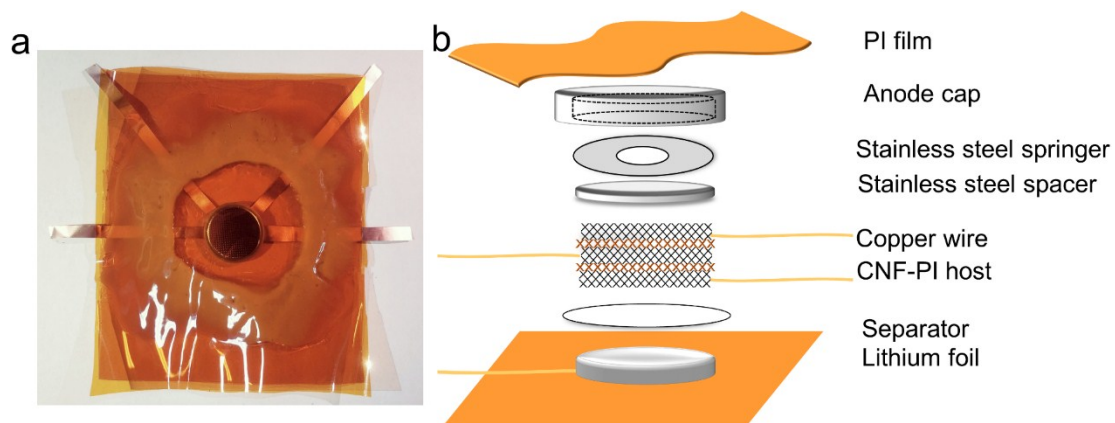


Fig. S6. (a) Digital photos of the voltage monitoring cell and (b) the schematic illustration of its inside structure. Three copper wire terminals link separately three layers of CNF in the CNF-PI host to monitor the voltage. The anode cap and stainless-steel springer/spacer are assembled to fix the cell and release the packaging stress.

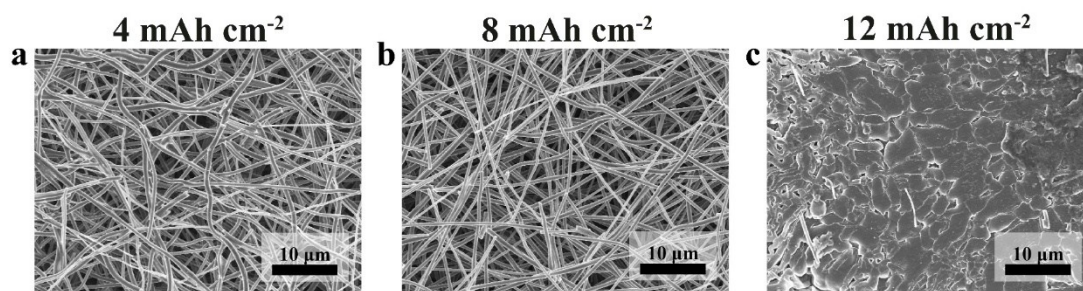


Fig. S7. (a-c) SEM images of the CNF-PI host when (a) 4 mAh cm^{-2} , (b) 8 mAh cm^{-2} , (c) 12 mAh cm^{-2} lithium was plated in. Only carbon nanofibers are observed on the surface until the lithium deposition capacity increasing to 12 mAh cm^{-2} .

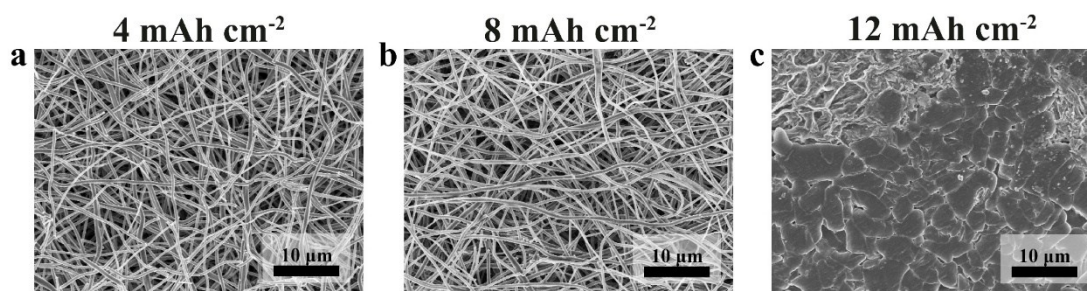


Fig. S8. (a-c) SEM images of lithium depositing inside the CNF-PI host after 10 cycles at 1 mA cm^{-2} and (b) 4 mAh cm^{-2} , (b) 8 mAh cm^{-2} , (c) 12 mAh cm^{-2} .

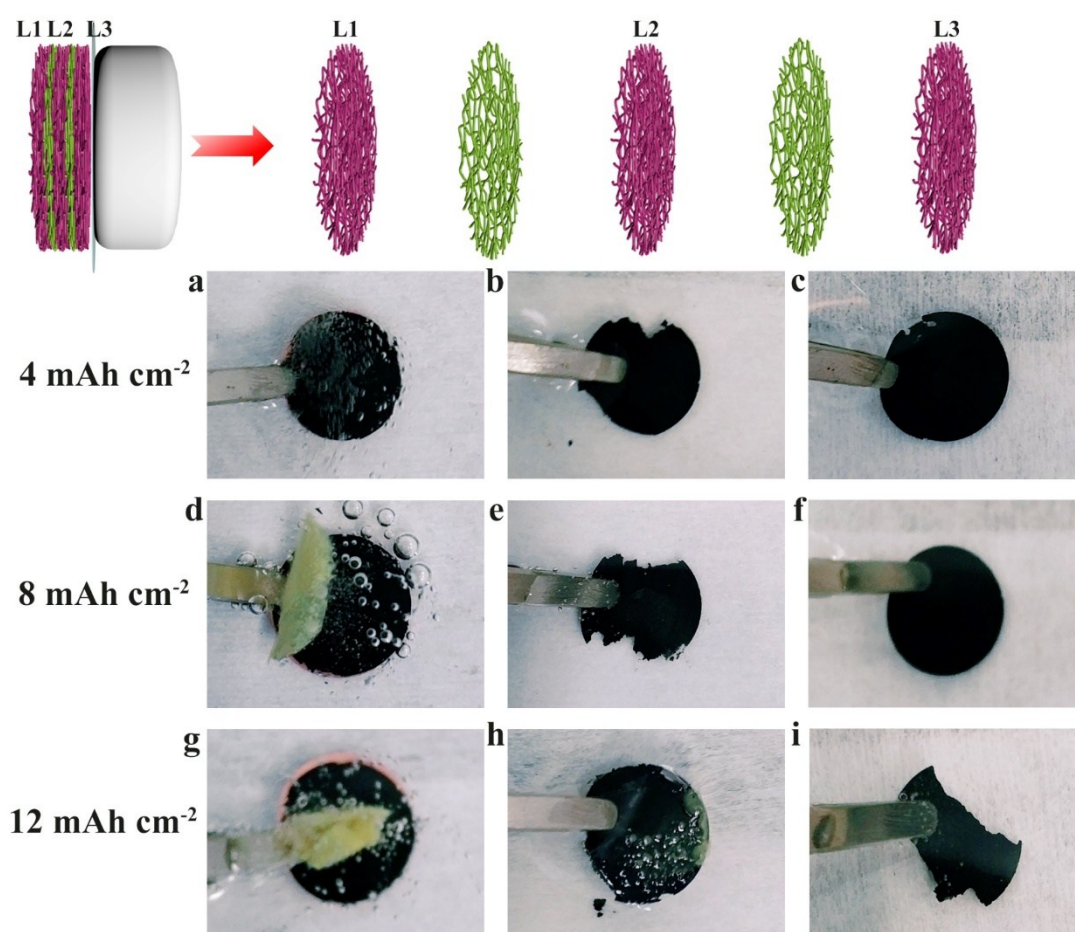


Fig. S9. CNF-PI host with (a, b, c) 4 mAh cm^{-2} , (d, e, f) 8 mAh cm^{-2} , (a, h, i) 12 mAh cm^{-2} lithium deposition was separated, and the (a, d, g) bottom, (b, e, h) intermediate, (c, f, i) top layer of CNF was dipped in water-alcohol mix solution. Bubbles generating at different lithium plating capacity confirm the stepwise deposition of lithium metal layer by layer inside the CNF-PI framework and the change in the monitoring voltage of the conductive layer reflecting the location of the lithium metal.

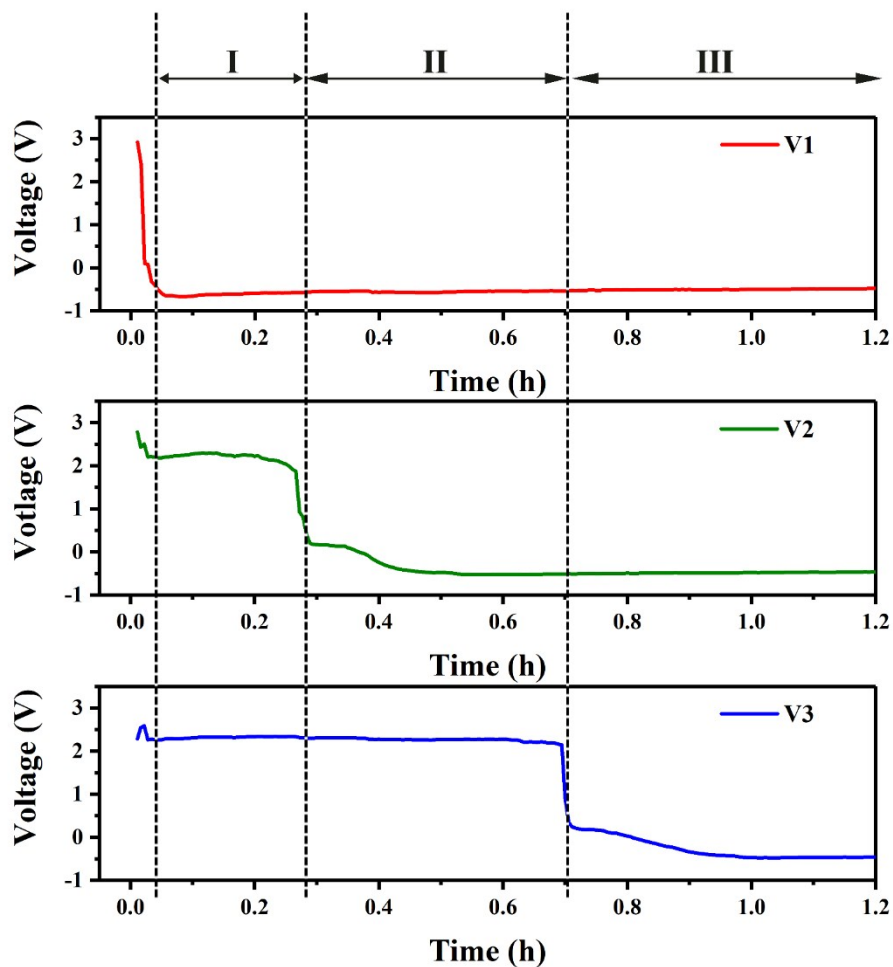


Fig. S10. Voltage profile of three layers of CNF monitoring voltage V1, V2 and V3 when a current of 10 mA cm^{-2} was applied.

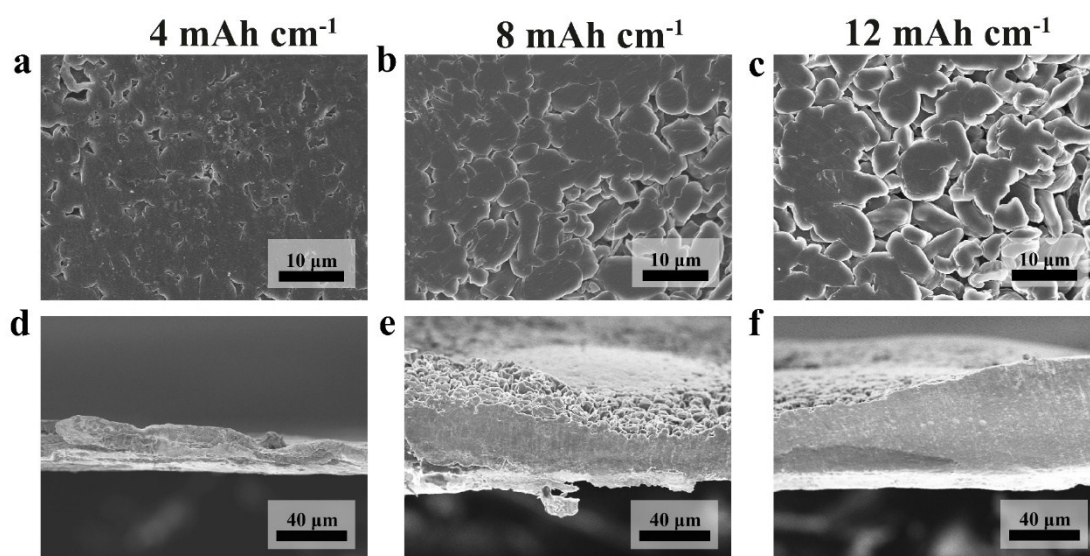


Fig. S11. (a-c) SEM images of lithium depositing on the Cu host when (a) 4 mAh cm^{-2} , (b) 8 mAh cm^{-2} , (c) 12 mAh cm^{-2} lithium was plated in. (d-f) Cross-sectional SEM images of lithium depositing on the Cu host when (d) 4 mAh cm^{-2} , (e) 8 mAh cm^{-2} , (f) 12 mAh cm^{-2} lithium was plated in.

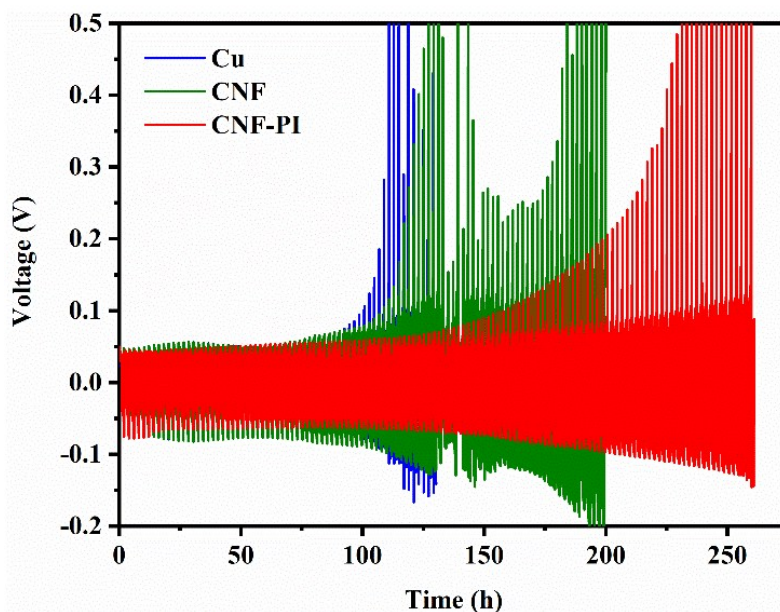


Fig. S12. Voltage-time profile of the half cells (Cu||Li, CNF||Li, CNF-PI||Li) at 3 mA cm⁻², 3 mAh cm⁻².

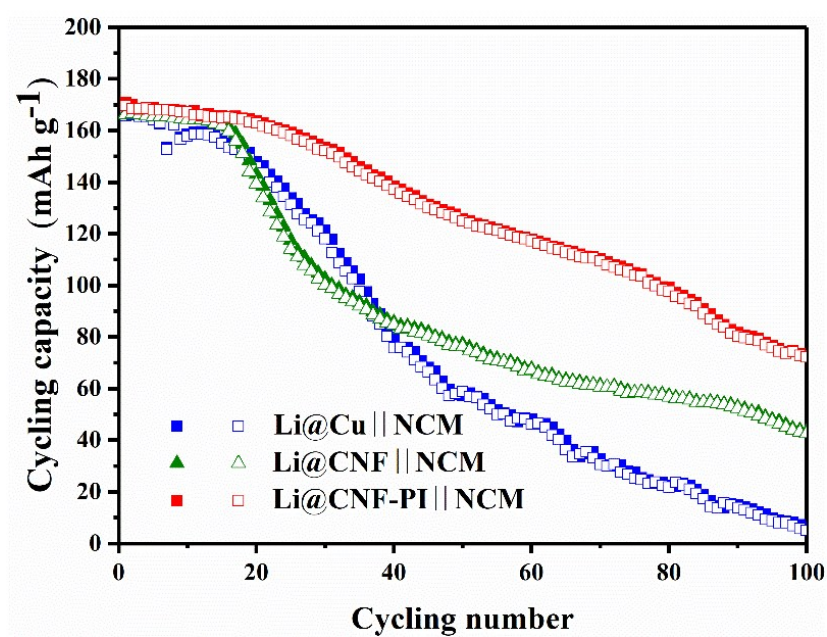


Fig. S13. Cycle performance of the full cell at 1 C (200 mA g⁻²) with 5 mAh cm⁻² lithium inserted.

Table S1. Comparison of Li plating/stripping CE of various hosts

	Host Materials	Host Thickness (μm)	Electrolyte	Cycling Capacity (mAh cm^{-2})	Current Densities (mA cm^{-2})	Coulombic Efficiency	Cycles
This work	CNF-PI	160	1 M LiPF ₆ in EC/DEC/DMEC + 10.0% FEC	3	1	97.5%	140
				3	3	96.2%	90
				5	3	96.6%	60
				10	5	96.5%	30
2017. Adv. Mater. ¹	Graphitized carbon fibers	1000	1 M LiTFSI in DOL/DME + 1% LiNO ₃	8	0.5	~98%	70
2017. Joule. ²	Hollow carbon fiber	165	1 M LiTFSI in DOL/DME + 1% LiNO ₃	2	1	99.5%	240
2018. Adv. Energy Mater. ³	N-doped graphene modified 3D porous Cu	70	1 M LiTFSI in DOL/DME + 1% LiNO ₃	2	1	97%	50
2018. Adv. Energy Mater. ⁴	Porous poly-melamine-formaldehyde (PMF)	~200	1 M LiTFSI in DOL/DME	3	1	97.5	120
2018. Adv. Mater. ⁵	Carbon nanotube	~80	1 M LiTFSI in DOL/DME	5	1	97.5	100
2018. Adv. Mater. ⁶	Cu-CuO-Ni	~200	1 M LiTFSI in DOL/DME + 1% LiNO ₃	1	1	95%	250
2019. ESM. ⁷	Gold nanoparticle-modified carbon paper	137.1	1 M LiTFSI in DOL/DME + 1% LiNO ₃	1	2	97.6%	100
2019. Adv. Mater. ⁸	Cu nanowire	36.6	1 M LiTFSI in DOL/DME + 1% LiNO ₃	3	1	97.5%	60
2019. Nat. Comm. ⁹	Al ₂ O ₃ -Ni-Au	70	1 M LiTFSI in DOL/DME + 1% LiNO ₃	2	0.5	97 %	350

Supplementary References

1. T. T. Zuo, X. W. Wu, C. P. Yang, Y. X. Yin, H. Ye, N. W. Li and Y. G. Guo, *Advanced materials*, 2017, **29**.
2. L. Liu, Y.-X. Yin, J.-Y. Li, N.-W. Li, X.-X. Zeng, H. Ye, Y.-G. Guo and L.-J. Wan, *Joule*, 2017, **1**, 563-575.
3. R. Zhang, S. Wen, N. Wang, K. Qin, E. Liu, C. Shi and N. Zhao, *Advanced Energy Materials*, 2018, **8**, 1800914.
4. L. Fan, H. L. Zhuang, W. Zhang, Y. Fu, Z. Liao and Y. Lu, *Advanced Energy Materials*, 2018, **8**, 1703360.
5. Z. Sun, S. Jin, H. Jin, Z. Du, Y. Zhu, A. Cao, H. Ji and L. J. Wan, *Advanced materials*, 2018, **30**, e1800884.
6. S. Wu, Z. Zhang, M. Lan, S. Yang, J. Cheng, J. Cai, J. Shen, Y. Zhu, K. Zhang and W. Zhang, *Advanced materials*, 2018, **30**.
7. B. Hong, H. Fan, X.-B. Cheng, X. Yan, S. Hong, Q. Dong, C. Gao, Z. Zhang, Y. Lai and Q. Zhang, *Energy Storage Materials*, 2019, **16**, 259-266.
8. C. Zhang, R. Lyu, W. Lv, H. Li, W. Jiang, J. Li, S. Gu, G. Zhou, Z. Huang, Y. Zhang, J. Wu, Q. H. Yang and F. Kang, *Advanced materials*, 2019, DOI: 10.1002/adma.201904991, e1904991.
9. J. Pu, J. Li, K. Zhang, T. Zhang, C. Li, H. Ma, J. Zhu, P. V. Braun, J. Lu and H. Zhang, *Nature communications*, 2019, **10**, 1896.